ICIC Express Letters
Volume **15**, Number **8**, August **2021**

ICIC International ©2021 ISSN 1881-803X
pp. **887–895**

ECG NOISE CLASSIFICATION USING CEEMDAN AND MULTILAYER PERCEPTRON

Andrew and Sani Muhamad Isa

Computer Science Department, BINUS Graduate Program – Master of Computer Science
Bina Nusantara University
JL. K. H. Syahdan No. 9, Kemanggisan, Palmerah, Jakarta 11480, Indonesia
{ andrew014; sani.m.isa }@binus.ac.id

Received November 2020; accepted February 2021

Abstract. *As one of the most common signals utilized in the medical field, Electrocardiogram (ECG) can be contaminated with various noises and should be denoised prior to medical analysis. Since ECG denoising performance is dependent on the characteristic of noise, ECG noise needs to be classified beforehand. This study proposes a machine learning-based ECG noise classification system as an alternative to the existing decision rule-based system to handle unaccustomed noise intensities more robustly. In the proposed system, 10-second segments of ECG are decomposed using Complete Ensemble Empirical Mode Decomposition with Adaptive Noise (CEEMDAN) to obtain several sub-signals and extract their features. A Multilayer Perceptron (MLP) is trained and validated using these features to classify the ECG segments into six classes based on the occurrence of three noise classes: baseline wander, muscle artifact, and powerline interference. The system was evaluated on the MIT-BIH Arrhythmia Database and achieved the best performance for 0 dB signal-to-noise ratio with 88.56% average sensitivity, 88.5% average positive predictivity, and 81.43% average threat score. The overall result demonstrates the system's ability to maintain its performance effectively upon exposure to different high noise intensities without the need for manual threshold configuration.*
Keywords: Signal decomposition, Neural network, Baseline wander, Muscle artifact, Powerline interference

1. **Introduction.** Electrocardiogram (ECG) is a graph of voltage against time that records the electrical activity of the heart. As a signal, ECG is susceptible to noise. In practice, ECG noise is often classified based on its cause, such as baseline wander (caused by respiration), muscle artifact (caused by muscle contraction), and powerline interference (caused by electromagnetic interference). These noises can alter ECG morphology, hamper ECG readings, and subsequently produce high false alarm rates [1], which in the worst-case scenario, may lead to misdiagnosis of cardiac arrhythmias [2]. Thus, their removal is essential.

ECG denoising or noise reduction refers to the process of removing ECG noises while maintaining the original signal. Over the years, numerous ECG denoising methods have been proposed, including adaptive filtering [3], wavelet transform thresholding [4], empirical mode decomposition [5], and machine learning-based methods [6,7]. ECG denoising requires different strategies for different noise classes [3]. While some methods are proven effective in denoising certain noise classes [8], a denoising model might be suitable only for denoising a particular noise class, so if the nature of the noise suddenly changes, the model needs to be readjusted or retrained [9]. Such premises indicate that the performance of most ECG denoising methods is dependent on the noise class. Hence to select the most appropriate set of denoising methods, ECG noise needs to be identified and classified in advance [2].

DOI: 10.24507/icicel.15.08.887

Only a few studies have explored ECG noise classification based on its cause. Satija et al. [2] presented an ECG noise classification system based on CEEMDAN and decision rules to classify ECG into six classes according to the presence of baseline wander, muscle artifact, and powerline interference. However, decision rules induce a less adaptive classification since they rely on preconfigured thresholds that might not accommodate unaccustomed noise intensities. This study aims to provide academic contributions by replacing the decision rules with MLP. As a machine learning-based classifier, MLP can learn from data and eliminate manual threshold configuration to overcome the downside of decision rules. In summary, the proposed system will receive 10-second segments of ECG with varying noise intensities as its input, decompose them using CEEMDAN to obtain features, and then utilize them to train and validate an MLP capable of classifying the ECG segments according to the occurrence of baseline wander, muscle artifact, and powerline interference.

The rest of this paper is organized as follows: Section 2 lists literature and works related to the study; Section 3 elaborates the proposed system and methodology; Section 4 discusses the evaluation results; Section 5 concludes the study and offers suggestions for future works.

2. Literature Review and Related Works.

2.1. **ECG noise.** Due to its ability to convey electrical information over time, ECG can be considered a signal, and therefore is prone to noise. Noise is defined as an undesired signal disturbance that might happen during acquisition, storage, transmission, processing, or conversion [10]. Many ECG-related studies, such as [8,11,12], classify ECG noise according to its cause, as shown in Figure 1. Three of the most popular noise classes are

a) **Baseline Wander (BW).** BW is mainly caused by respiratory activity. It is characterized by baseline drift with a frequency spectrum of 0.05-1 Hz and amplitude about 15% of peak-to-peak ECG amplitude. Due to its nature, BW may cause problems in ECG peak detection.

b) **Muscle Artifact (MA).** MA, also known as Electromyographic (EMG) noise, is mainly caused by contractions of other muscles in the vicinity of the electrode contact. Its frequency ranges from 0 to 10 kHz, and its amplitude is about 10% of peak-to-peak ECG amplitude.

c) **Powerline Interference (PLI).** PLI is mainly caused by electromagnetic interference in contact between the ECG machine and other electrical equipment such as cables or power supplies. PLI amplitude is up to 50% of peak-to-peak ECG amplitude. PLI frequency spectrum is either 50 or 60 Hz, depending on the utility frequency of countries.

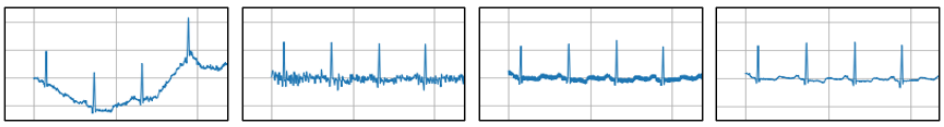

FIGURE 1. ECG continuously corrupted with (a) BW, (b) MA, and (c) PLI – in comparison with (d) their noise-free counterpart

2.2. **Complete Ensemble Empirical Mode Decomposition with Adaptive Noise (CEEMDAN).** CEEMDAN is an EMD-based signal decomposition method. It was introduced by Torres et al. [13] as an improvement to its predecessors: Empirical Mode Decomposition (EMD) [14] and Ensemble EMD (EEMD) [15]. Consequently, the CEEMDAN algorithm is based on EMD – it decomposes a signal into a set of intrinsic oscillatory components known as Intrinsic Mode Functions (IMFs). Each IMF represents the original

signal in decreasing order of frequencies: The first IMF captures the highest frequency and the following IMFs capture lower frequencies. CEEMDAN algorithm is also based on EEMD – different realizations of white Gaussian noise are added to the original signal over an ensemble of trials. However, unlike EEMD, which decomposes every realization independently and produces their respective residues, CEEMDAN averages the decomposition results of each realization to assemble a unique residue. As a result, CEEMDAN resolves the drawbacks of both EMD (e.g., mode mixing – multiple IMFs capture the same frequency or multiple frequencies are captured by a single IMF) and EEMD (e.g., incompleteness – unable to reconstruct the original signal). Moreover, CEEMDAN offers lower computational cost compared to EEMD. Due to these advantages, CEEMDAN is currently considered a state-of-the-art signal decomposition method.

2.3. **Multilayer Perceptron (MLP).** MLP is one of the simplest, most common neural network models for conducting regression or classification. As a neural network, MLP is a constituent of soft computing (i.e., a set of methodologies that tolerates imprecision and uncertainty to provide low-cost solutions, tractability, and robustness [16]). The architecture of MLP consists of input, hidden, and output layers, as illustrated in Figure 2. Each layer is composed of nodes (neurons) for storing information. MLP is fully connected – each node in one layer connects to every node in the next layer through weighted connections. There are two learning algorithms used by MLP: forward propagation, which involves propagating the inputs towards the output nodes, calculating output, and computing error by comparing the output with the target; backpropagation, which is performed afterwards by updating all connection weights using gradient descent to reduce the error. Both algorithms share the same goal: to provide the network with the most optimal weight combination.

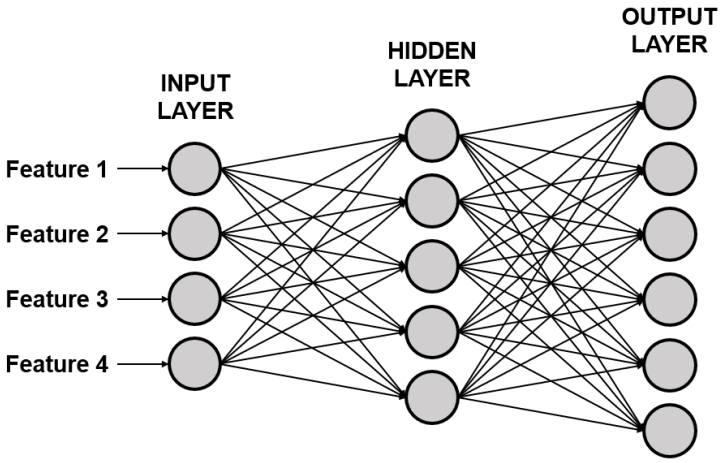

FIGURE 2. An MLP architecture incorporating four input nodes, one hidden layer with five nodes, and six output nodes

2.4. **Related works.** Most studies, such as [17,18], classified ECG as noise-free or noisy. Others, such as [19,20], classified ECG into multiple levels based on noise intensity. They did so to assess ECG quality. Only a few have explored ECG noise classification based on its cause. As the primary reference of this study, Satija et al. [2] proposed an automated ECG noise classification system for unsupervised healthcare monitoring. The system incorporates CEEMDAN as the signal decomposition method to obtain features and decision rules as the classifier to classify 10-second segments of ECG into six classes: clean, BW, MA, PLI, BW+MA, and BW+PLI. The system was evaluated on many datasets, including the MIT-BIH Arrhythmia Database, and achieved 98.93% average sensitivity,

98.39% average positive predictivity, and 97.38% average threat score. Such high performance is unsurprising since decision rules work by manually tweaking decision parameters (thresholds) to fit as much data as possible. However, it creates a less adaptive classification system – the thresholds need to be reconfigured based on the acceptable maximum noise level [2], which is impractical considering realistic ECG noise can manifest in various intensities [12].

3. **Proposed System and Methodology.** This study proposes a machine learning-based ECG noise classification system with two main components: CEEMDAN as the signal decomposition method and MLP as the classifier. Figure 3 displays the substantial flow of the proposed system. Initially, the system accepts 10-second segments of ECG with various noise intensities as its input. Each ECG segment is preprocessed, and then decomposed using CEEMDAN to obtain a set of IMFs and residues, which are used to compute High-Frequency (HF) and Low-Frequency (LF) signals. Then, several features involving Standard Deviation (STD), Number of Zero-Crossings (NZC), and Autocorrelation Function (ACF) are extracted from these signals. By then, each ECG segment is represented by one feature vector. All feature vectors are subsequently preprocessed and resampled into training and testing sets. An MLP is trained and validated by utilizing the training set. This MLP is used to predict the labels of every feature vector within the testing set. The predicted labels are compared with the actual ones to compute several performance metrics for evaluation purposes. Meanwhile, the methodology to develop the system can be divided into five core stages.

3.1. **Dataset collection.** The noise-free ECG dataset, also called the clean dataset, was acquired from the MIT-BIH Arrhythmia Database [21]. The database consists of 48 half-hour two-leads ambulatory ECG recordings, each digitized at 360 samples per second.

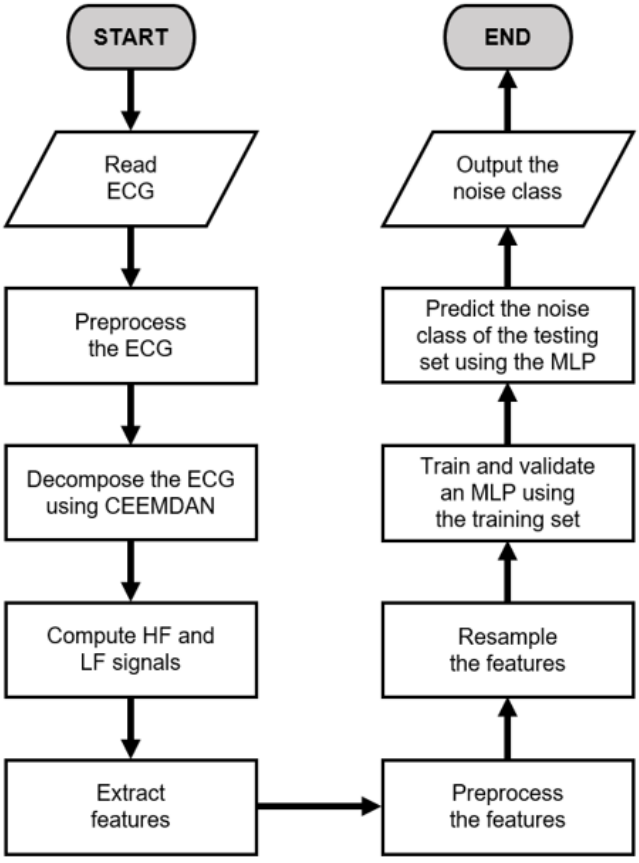

FIGURE 3. A flowchart summarizing the proposed system

The beats, rhythm, and signal quality were labeled by cardiologists. The clean dataset was acquired from Records 100, 102, 113, 123, 213, 219, and 231 since they do not possess any noise-related annotations. Meanwhile, the ECG datasets corrupted with BW or MA, also called the BW/MA datasets, were generated synthetically by injecting noise signals obtained from the MIT-BIH Noise Stress Test Database [12]. The database contains 12 half-hour ECG recordings and three half-hour noise recordings. Both BW and MA noise recordings were injected into the clean dataset to generate the BW/MA datasets in various intensities.

3.2. **Dataset preprocessing.** Each dataset was preprocessed by performing the following procedure: 1) centering the data (i.e., changing their mean to zero); 2) splitting the data per 10 seconds. The creation of ECG datasets corrupted with PLI, also called the PLI datasets, was conducted after data centering but before data splitting. It was performed by simply adding a cosine wave with calibrated amplitude, as demonstrated by Lin and Hu [22].

3.3. **Feature extraction.** Each ECG segment was subjected to the feature extraction stage adapted from Satija et al. [2]. Initially, every 10-second segment of ECG was decomposed using CEEMDAN, producing a set of IMFs and residues, as illustrated in Figure 4. For each segment, the first three IMFs were summed to form an HF signal that may capture HF noises, including MA and PLI, whereas the first residue that meets the specified stopping condition (NZC <= 10, considering 1 Hz baseline drift) acted as an LF signal that may capture LF noises including BW. Figure 5 exhibits several examples of HF and LF signals. From these signals, four features were extracted: 1) STD of the HF signal; 2) total duration of the gate signal's local pulses based on NZC of the HF signal; 3) average first local maximum ACF of the first IMF frames of the HF signal; 4) STD of the LF signal. For additional information regarding the features, please refer to the original study [2]. In this study, however, amplitude-based features were replaced by STD since the important parameter used in signal operations is power, not amplitude [23]. Finally, the features were combined to form a feature vector, which in turn constitutes a feature set.

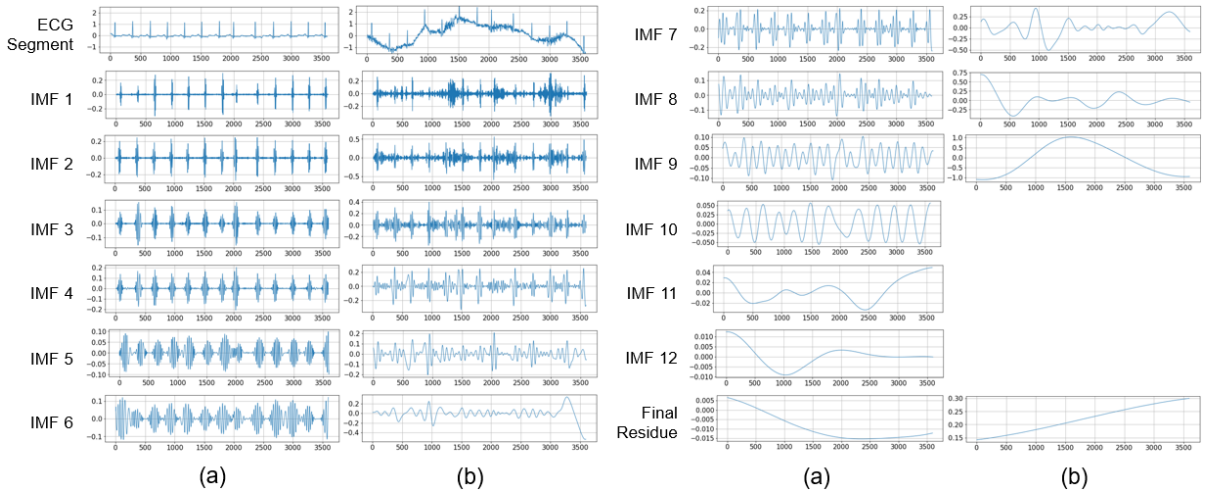

FIGURE 4. The CEEMDAN decomposition of (a) a noise-free ECG and (b) an ECG corrupted with BW+MA

3.4. **Feature preprocessing and resampling.** Each feature set was preprocessed by performing the following procedure: 1) assigning labels according to which noise class the feature vector represents, as presented in Table 1; 2) normalizing features by scaling them to a range of 0 and 1, as demonstrated by Noor et al. [24]. Then, the normalized feature

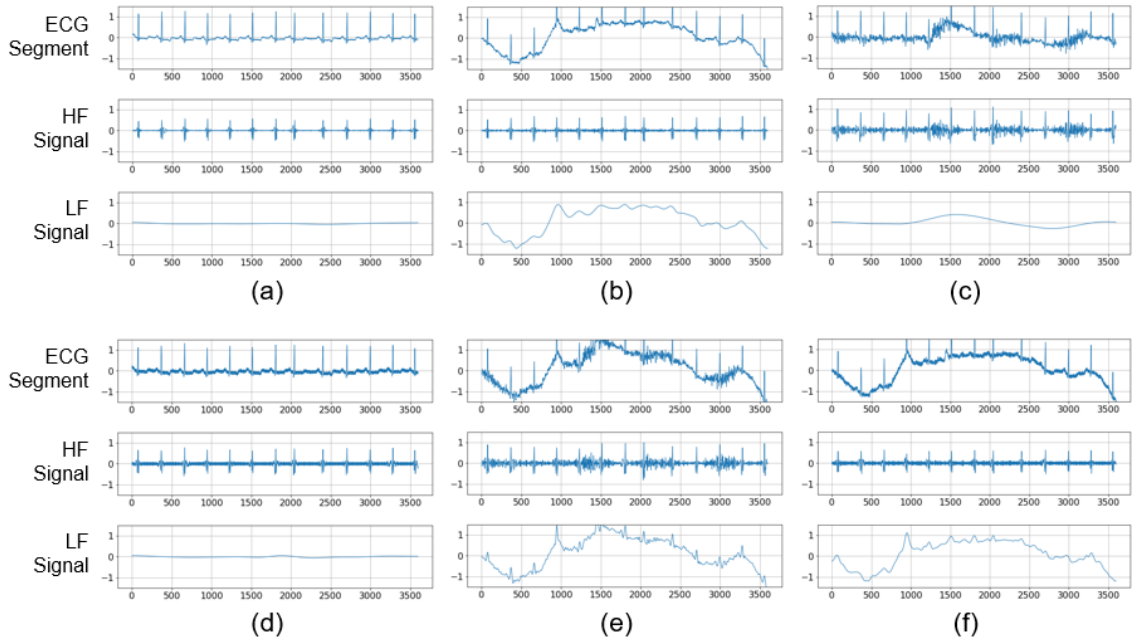

FIGURE 5. The HF and LF signals of (a) a noise-free ECG and (b) ECG corrupted with BW, (c) MA, (d) PLI, (e) BW+MA, and (f) BW+PLI

TABLE 1. The label assignment of the six noise classes

Noise class	Description	Label
Clean	A noise-free ECG segment.	0
BW	An ECG segment corrupted with baseline wander.	1
MA	An ECG segment corrupted with muscle artifact.	2
PLI	An ECG segment corrupted with powerline interference.	3
BW+MA	An ECG segment corrupted with baseline wander and muscle artifact.	4
BW+PLI	An ECG segment corrupted with baseline wander and powerline interference.	5

sets were resampled by splitting them into training and testing sets with a ratio of 80 against 20.

3.5. **Training and validation.** Each training set was subjected to 10-fold cross-validation and grid search. Table 2 lists the hyperparameter values to be searched. While most values were determined according to best practices, the number of hidden layers was set to one since deeper neural networks are more likely to overfit [25]. The hyperparameter combination with the highest validation score was incorporated into the MLP architecture.

4. **Results and Discussion.** The system was evaluated on the MIT-BIH Arrhythmia Database, utilizing the testing set defined in Section 3.4. The MLP received every feature vector within the testing set and predicted their corresponding labels. The predicted labels were compared with the actual ones to determine the number of true positives TP, false positives FP, and false negatives FN for every class. Based on these statistics, several performance metrics were computed, including sensitivity Se, positive predictivity Pp, and threat score Ts, each defined as follows: $Se = \frac{TP}{TP+FN} \times 100\%$, $Pp = \frac{TP}{TP+FP} \times 100\%$, and $Ts = \frac{TP}{TP+FP+FN} \times 100\%$. The classification performance was measured using the macro-average score (i.e., averaging the score of all classes) of each metric. A confusion matrix was also computed to provide additional insight. Table 3 summarizes the system's

Table 2. The hyperparameter values searched upon the grid search

Hyperparameter	Values
Hidden layer size	[one layer with nodes equal to the average of the number of input and output nodes]
Activation function	[logistic sigmoid, hyperbolic tangent sigmoid, Rectified Linear Unit]
Solver	[stochastic gradient descent, adaptive moment estimation]
Learning rate	$[0.01, 0.001]$
Batch size	$[2, 4, 32]$
Number of epochs	[1000]

Table 3. The classification performance summary of the proposed system

Noise intensity (signal-to-noise ratio)	Average sensitivity (%)	Average positive predictivity (%)	Average threat score (%)
−6 dB	87.83	87.93	80.85
0 dB	**88.56**	**88.5**	**81.43**
6 dB	86.24	86.43	78.15
12 dB	85.38	85.7	76.7
18 dB	80.56	80.65	69.14
24 dB	57.21	57.74	40.22

Table 4. The confusion matrix for the 0 dB SNR classification

		Predicted					
		Clean	**BW**	**MA**	**PLI**	**BW+MA**	**BW+PLI**
Actual	**Clean**	252	0	0	0	0	0
	BW	0	228	8	0	16	0
	MA	0	10	187	0	55	0
	PLI	0	0	0	251	0	1
	BW+MA	0	24	53	0	175	0
	BW+PLI	0	0	0	4	2	246

classification performance, while Table 4 visualizes the confusion matrix for the 0 dB Signal-to-Noise Ratio (SNR) classification.

Every ECG segment was classified into six classes: clean, BW, MA, PLI, BW+MA, and BW+PLI. Such classification is intended to provide a rough performance comparison with Satija et al.'s decision rule-based system [2]. According to Table 3, the proposed system scores lower. The transition from decision rules (hard computing) to MLP (soft computing) possibly reduces the system performance due to soft computing's approximation and stochastic nature. However, they provide the system with better capabilities to handle real-world problems. In this case, the MLP's forward and backpropagation now automate the threshold configuration process by readjusting the weights to maintain the system performance effectively upon receiving unaccustomed, realistic data.

The classification was conducted with various noise intensities to reveal whether they affect the performance of a machine learning-based system. Apparently, they do – lower noise intensities (higher SNR) result in slightly lower performance. Low noise intensity establishes less distorted ECG, which are more similar to noise-free ECG in terms of feature and morphology. As a result, distinguishing them becomes more difficult. At 24 dB SNR, the noise classes become barely distinguishable, causing significantly poor performance. Still, the performance does not abruptly change when the system is exposed to different

high noise intensities, highlighting the system's robustness in handling unaccustomed noise intensities.

The confusion matrix reveals the detailed classification result for the best performing noise intensity (0 dB SNR). It is shown that despite the 81.43% average threat score, the system demonstrated satisfying performance in classifying individual noises. The system rarely confused BW with MA but never confused them with PLI. The BW/MA confusion occurs because they share the same traits (i.e., baseline drift and HF disturbances), albeit at different levels. Meanwhile, a composite noise and its components are very similar in terms of features. The introduction of BW+MA as a composite noise thus creates additional confusion (i.e., between BW+MA and BW and between BW+MA and MA), causing a significant performance decline.

5. **Conclusion and Future Works.** This study proposes a novel ECG noise classification system based on CEEMDAN and MLP. The system can classify well-known ECG noises, such as BW, MA, and PLI, in various intensities to support ECG denoising and analysis. The system was evaluated on the MIT-BIH Arrhythmia Database. The best performance was obtained for 0 dB SNR with 88.56% average sensitivity, 88.5% average positive predictivity, and 81.43% average threat score. The result demonstrates how the proposed system no longer requires manual threshold configuration to maintain its performance effectively upon exposure to different high noise intensities, thus concluding that the system is more robust in handling unaccustomed, realistic noise intensities. Future works of this study would be enhancing the system by optimizing the features, exploring recent machine learning models, or expanding the scope to include other kinds of ECG noise.

REFERENCES

[1] Q. Li and G. D. Clifford, Signal quality and data fusion for false alarm reduction in the intensive care unit, *J. Electrocardiol.*, vol.45, no.6, pp.596-603, 2012.

[2] U. Satija, B. Ramkumar and M. S. Manikandan, Automated ECG noise detection and classification system for unsupervised healthcare monitoring, *IEEE J. Biomed. Heal. Informatics*, vol.22, no.3, pp.722-732, 2017.

[3] N. V. Thakor and Y.-S. Zhu, Applications of adaptive filtering to ECG analysis: Noise cancellation and arrhythmia detection, *IEEE Trans. Biomed. Eng.*, vol.38, no.8, pp.785-794, 1991.

[4] M. Alfaouri and K. Daqrouq, ECG signal denoising by wavelet transform thresholding, *Am. J. Appl. Sci.*, vol.5, no.3, pp.276-281, 2008.

[5] M. Blanco-Velasco, B. Weng and K. E. Barner, ECG signal denoising and baseline wander correction based on the empirical mode decomposition, *Comput. Biol. Med.*, vol.38, no.1, pp.1-13, 2008.

[6] K. Antczak, Deep recurrent neural networks for ECG signal denoising, *arXiv.org*, arXiv: 1807.11551, 2018.

[7] C. T. C. Arsene, R. Hankins and H. Yin, Deep learning models for denoising ECG signals, *2019 the 27th European Signal Processing Conference (EUSIPCO)*, pp.1-5, 2019.

[8] S. L. Joshi, R. A. Vatti and R. V. Tornekar, A survey on ECG signal denoising techniques, *2013 International Conference on Communication Systems and Network Technologies*, pp.60-64, 2013.

[9] J. Guan, R. Li, R. Li, W. Li, J. Wang and G. Xie, Automated dynamic electrocardiogram noise reduction using multilayer LSTM network, *Proc. of the 15th EAI International Conference on Mobile and Ubiquitous Systems: Computing, Networking and Services*, pp.197-206, 2018.

[10] V. Tuzlukov, *Signal Processing Noise*, CRC Press, 2018.

[11] H. Limaye and V. V. Deshmukh, ECG noise sources and various noise removal techniques: A survey, *Int. J. Appl. or Innov. Eng. Manag.*, vol.5, no.2, pp.86-92, 2016.

[12] G. B. Moody, W. K. Muldrow and R. G. Mark, A noise stress test for arrhythmia detectors, *Comput. Cardiol.*, vol.11, pp.381-384, 1984.

[13] M. E. Torres, M. A. Colominas, G. Schlotthauer and P. Flandrin, A complete ensemble empirical mode decomposition with adaptive noise, *2011 IEEE International Conference on Acoustics, Speech and Signal Processing (ICASSP)*, pp.4144-4147, 2011.

[14] N. E. Huang et al., The empirical mode decomposition and the Hilbert spectrum for nonlinear and non-stationary time series analysis, *Proc. of R. Soc. A Math. Phys. Eng. Sci.*, vol.454, pp.903-995, 1998.

[15] Z. Wu and N. E. Huang, Ensemble empirical mode decomposition: A noise assisted data analysis method, *Adv. Adapt. Data Anal.*, vol.1, no.1, pp.1-41, 2009.

[16] L. A. Zadeh, Soft computing and fuzzy logic, in *Fuzzy Sets, Fuzzy Logic, and Fuzzy Systems: Selected Papers by Lotfi A. Zadeh*, G. J. Klir and B. Yuan (eds.), World Scientific Publishing Company, 1996.

[17] J. Behar, J. Oster, Q. Li and G. D. Clifford, ECG signal quality during arrhythmia and its application to false alarm reduction, *IEEE Trans. Biomed. Eng.*, vol.60, no.6, pp.1660-1666, 2013.

[18] C. Orphanidou, T. Bonnici, P. Charlton, D. Clifton, D. Vallance and L. Tarassenko, Signal quality indices for the electrocardiogram and photoplethysmogram: Derivation and applications to wireless monitoring, *IEEE J. Biomed. Heal. Informatics*, vol.19, no.3, pp.832-838, 2015.

[19] S. I. Haider and M. Alhussein, Detection and classification of baseline-wander noise in ECG signals using discrete wavelet transform and decision tree classifier, *Elektron. ir Elektrotechnika*, vol.25, no.4, pp.47-57, 2019.

[20] Q. Li, C. Rajagopalan and G. D. Clifford, A machine learning approach to multi-level ECG signal quality classification, *Comput. Methods Programs Biomed.*, vol.117, no.3, pp.435-447, 2014.

[21] G. B. Moody and R. G. Mark, The impact of the MIT-BIH arrhythmia database, *IEEE Eng. Med. Biol. Mag.*, vol.20, no.3, pp.45-50, 2001.

[22] Y.-D. Lin and Y. H. Hu, Power-line interference detection and suppression in ECG signal processing, *IEEE Trans. Biomed. Eng.*, vol.55, no.1, pp.354-357, 2008.

[23] S. W. Smith, *The Scientist and Engineer's Guide to Digital Signal Processing*, 2nd Edition, California Technical Publishing, San Diego, 1999.

[24] C. W. M. Noor, R. Mamat and A. N. Ahmed, Comparative study of artificial neural network and mathematical model on marine diesel engine performance prediction, *International Journal of Innovative Computing, Information and Control*, vol.14, no.3, pp.959-969, 2018.

[25] T. L. Dang, T. Cao and Y. Hoshino, Classification of metal objects using deep neural networks in waste processing line, *International Journal of Innovative Computing, Information and Control*, vol.15, no.5, pp.1901-1912, 2019.